

Design of a CPW fed simple hexagonal shape UWB antenna with WLAN and WiMAX band rejection characteristics

Tapan Mandal · Santanu Das

Published online: 25 December 2014
© Springer Science+Business Media New York 2014

Abstract This article presents a coplanar waveguide fed regular hexagonal antenna for ultra wide bandwidth (UWB). Then this antenna is modified to obtain band rejection for the wireless local area network of 5.15–5.825 GHz (IEEE 802.11a) and wireless microwave access of 3.3–3.7 GHz (IEEE 802.16) by incorporating U-shape slots within the hexagonal patch. Notch bands can easily be controlled by few geometry parameters of the U-slots. Return loss, impedance, gain and radiation characteristics of them are studied and discussed here. From the results, it has been observed that the antenna significantly satisfies the Federal Communication Commission's UWB frequency (3.1–10.6 GHz) range while showing the band rejection performance in the frequency bands of 3.3–3.7 and 5.12–5.9 GHz. The antenna gain varies from 2.6 to 6.4 dB over the whole operating band excluding the notch bands. Surface current distributions and transmission line model are used to analyze the effects of the slots. Measured group delay has very small variation within the operating band except notch bands and hence the proposed antenna may be suitable for UWB applications.

Keywords Hexagonal monopole · CPW fed · U-slot · UWB antenna · WLAN · WiMAX

T. Mandal (✉)
Department of Information Technology, Government College
of Engineering and Textile Technology, Hooghly,
Serampore 712201, India
e-mail: tapanmandal20@rediffmail.com

S. Das
Department of Electronics & Tele-Communication Engineering,
Bengal Engineering and Science University, Shibpur,
Howrah 711103, India
e-mail: santanumdas@yahoo.com

1 Introduction

In 2002, the US-Federal Communications Commission (US-FCC) approved the frequency band from 3.1 to 10.6 GHz for commercial communication applications [1]. Since then, considerable research efforts have been paid into ultra wide band (UWB) communication technology. This type of UWB antenna has been realized by using either microstrip line [2–5] or coplanar wave guide (CPW) [9–12] feeding structure. The UWB antenna has the advantages of low profile, light weight, wide BW, low cost, high data rate and good omnidirectional radiation pattern [2–8]. In particular, CPW fed have many salient features like less radiation loss, less dispersion, easy integration with monolithic microwave integrated circuits (MMIC). Therefore, CPW fed UWB antennas are currently under consideration for numerous applications such as remote sensing, radar, imaging, localization and medical applications.

Many of UWB antennas have been offered for various applications in the last decade [9–18]. Planar UWB monopole antennas with rectangular [9], disk [10, 11], elliptical [12], hexagonal [13] and triangular [14] shapes have been reported. The CPW fed hexagonal monopole antennas are found to have 10 dB return loss bandwidth for UWB application [13] with large size structure. Rectangular slot with resistive load hexagonal for GPR application have been demonstrated [15]. A compact hexagonal wide-slot antenna with microstrip-fed monopole for UWB application has been described in [2, 4] but its structure is either complex or large in size.

However, the existing wireless local area network (WLAN: IEEE 802.11a) and wireless microwave access (WiMAX: IEEE 802.16) service bands of 5.15–5.825 and 3.3–3.7 GHz are responsible for the performance degradation of UWB system because of the interference. To prevent this

problem, UWB with band rejection characteristic is desirable. In the conventional design, band stop filters are added to the end of the antenna. Thereby, the size of the antenna is increased. Several UWB antennas with band rejection characteristic have been proposed [3–8, 11, 14–17]. For printed monopole antennas, the most familiar methods to achieve band-notched function are etching slots on the metallic patch, feeder or ground plane [12–14] in different shapes such as C-shaped [9, 11], U-shaped [7], L-shaped [8], I-shaped [18] slot etc. The band notch performance is achieved by placing parasitic strips in close proximity to the antenna [6, 12]. From the literature survey, it is found that a CPW fed regular hexagonal monopole antenna (RHMA) with dual stop band has not been investigated in details so far. However, most of UWB antennas have no more than single notch band which reveal that potential interference from other narrow band may still exist.

In this paper, a CPW fed U-slot hexagonal monopole antenna with WLAN and WiMAX band notch characteristics has been proposed. The design initially begins with a regular hexagonal monopole antenna (RHMA). The desired band rejection characteristics are obtained by incorporating a pair of U-slots on the hexagonal radiating patch. All the simulations are carried out using Method of Moment (MoM) based IE3D simulation software [19]. In this paper all return loss, group delay and phase measurements are taken out by Agilent make Vector Network Analyzer (N5230A).

2 Antenna configuration

2.1 Prototype antenna geometry

The design initially begins with a regular hexagonal monopole antenna (RHMA). Figure 1 shows a configuration of the prototype antenna which has been printed on a substrate with dielectric constant (ϵ_r) = 4.4, height (h) = 1.59 mm, loss tangent ($\tan d$) = 0.002. It consists of a hexagonal patch, ground plane and CPW fed line on the same plane of the substrate. A 50 Ω CPW transmission line is designed with a strip width (W_f) of 3.8 mm.

The lower band edge frequency (f_l) has been determined for UWB using formulas [8, 10] given in Eq. (1)

$$f_l = \frac{c}{\lambda} = \frac{7.2}{(H + r + T)} \tag{1}$$

where H is the height from the ground plane edge to the top of the hexagon and r is the radius of an equivalent cylindrical monopole antenna in cm and T is the gap between the ground plane and patch in cm. With reference to configurations in Fig. 1 with side length (L_p), the dimensions of height (H) and radius (r) of the equivalent cylindrical monopole antenna

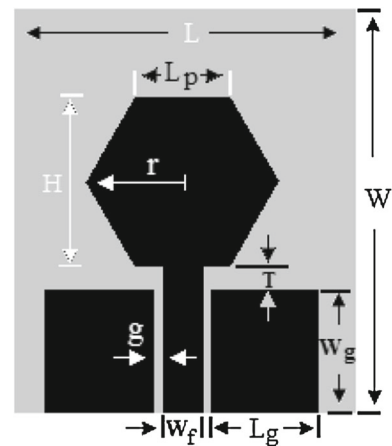


Fig. 1 Geometry of prototype antenna

are obtained (by equating their areas) as follows:

$$r = \frac{3L_p}{4\pi} \tag{2}$$

$$H = \sqrt{3}L_p \tag{3}$$

By selecting the value of $L_p = 13.6$ mm, the following parameters— r , H and f_l can be computed using the Eqs. (1)–(3). To cover the entire UWB frequency range, $T = 1.3$ mm, $L_g = 28$ mm and $W_g = 13.5$ mm are taken in the antenna design using MoM based simulator. The computed dimensions of the antenna parameters and selected parameters value using simulator are given in Table 1.

2.2 Band-notched antenna design

In order to obtain a notch band in the frequency range of 5.15–5.825 GHz, a thin U-slot is etched out from the RHMA (Fig. 2). Usually, the length of the slot is made approximately equal to half the guided wavelength at the notch frequency of the band. This is given by

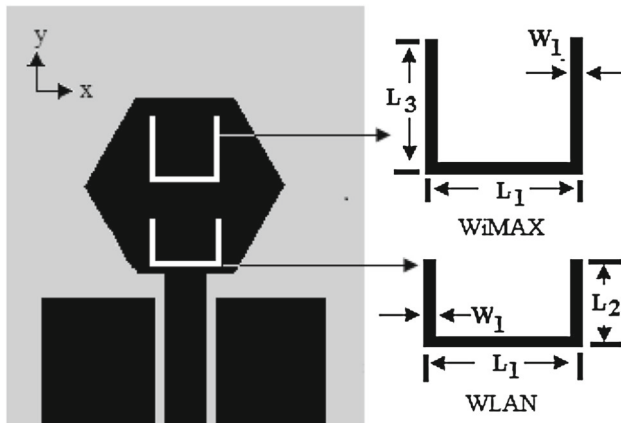
$$L_{total_WLAN} = \frac{\lambda_g}{2} = \frac{c}{2f_{notch_WLAN}\sqrt{\frac{\epsilon_r+1}{2}}} \tag{4}$$

$$L_{total_WLAN} = L_1 + 2L_2 \tag{5}$$

where L_{total_WLAN} is the total length of the slot. For the notch frequency $f_{notch_WLAN} = 5.5$ GHz, the length of the slot is calculated as 16.6 mm. The slot width is found to be 0.3 mm by way of simulation in order to achieve close to the exact notch band. In addition to this, WiMAX stop band is realized by inserting another narrow U-slot on the radiating RHMA. This U-slot also has a length of half wavelength at the desired notch frequency (3.5 GHz). For center notch $f_{notch_WiMAX} = 3.5$ GHz, the length of the slot can be determined as 26.15 mm. From Eq. (4), the total length of the U-shape slot may be obtained at the beginning of this

Table 1 Optimized parameter for the proposed antenna

Parameter	L	W	$r = L_p$	g	H	T	W_f	Lg	L_1	L_2	L_3	W_1
Dimension (mm)	36	42	13.6	0.5	23.45	1.375	4.1	11.4	10	3.85	9.35	0.3

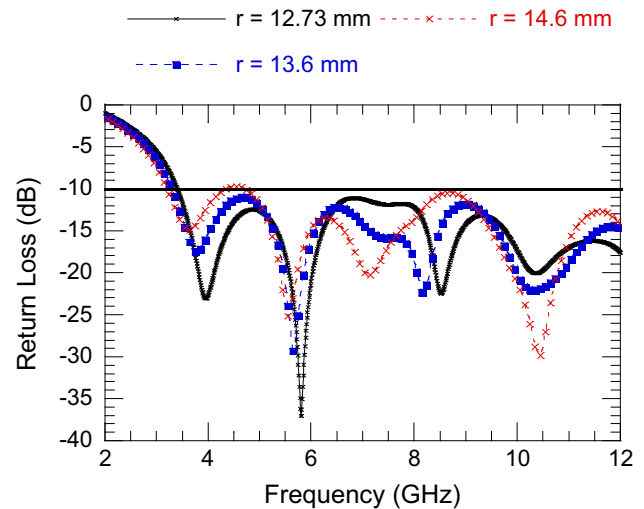
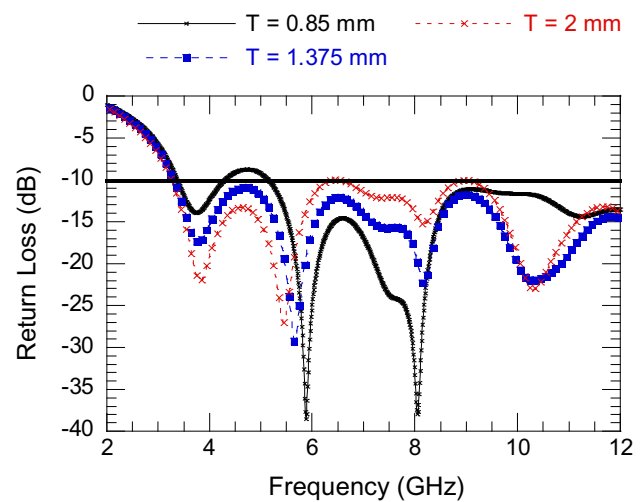
**Fig. 2** Geometry of proposed antenna

design. Finally the lengths are adjusted by using simulator for obtaining the desired results. The detailed dimensions are shown in Table 1.

3 Parametric study and observation

A parametric study is carried out to investigate the effects of the important parameters on the impedance matching. Figure 1 shows the configuration of the prototype antenna. It has mainly two parameters which are considered first for parametric study. Return loss characteristics for various radii of hexagonal patch are shown in Fig. 3. With the increase in radius of the patch, the lower edge frequency of the response moves toward the left side of the plot. The main reason is the increase of radius which in turn increases the height of the monopole antenna. Thus the patch plays a vital role for selecting the lower edge frequency of the band. The effects of extrusion depth T on the input impedance are simulated and shown in Fig. 4. From the result, it is observed that the gap between the ground plane and the radiating patch plays a significant role for impedance matching resulting in wide band. The gap creates a capacitance that neutralizes the inductive nature of the radiating patch to produce nearly-pure resistive input impedance.

The lower U-slot configuration on hexagonal patch has been used independently to obtain WLAN stop band. Here the return loss characteristics for various values of slot length (L_{total_WLAN}) and width (W_1) are shown in Figs. 5 and 6 respectively. It is observed from Fig. 5 that the notch band moves leftwards with higher peak as the length of U-slot

**Fig. 3** Simulated return loss for different radius (r)**Fig. 4** Simulated return loss for different extrusion depth (T)

is increased. Similarly, it is observed that an increase in width (W_1) of resonator results in moving leftwards of the center frequency of the notch. The slot length has greater impact than the slot width on shifting the frequency as is evident from Figs. 5 and 6. Therefore, the notch band of the proposed antenna can be easily controlled by the geometry parameters of the slot resonator. If the current distribution is observed, maximum current flows back to the feeding part due to the presence of U-slot inside the patch. Therefore negligible amount of currents is coupling to the patch and degenerates radiation around 5.15–5.93 GHz.

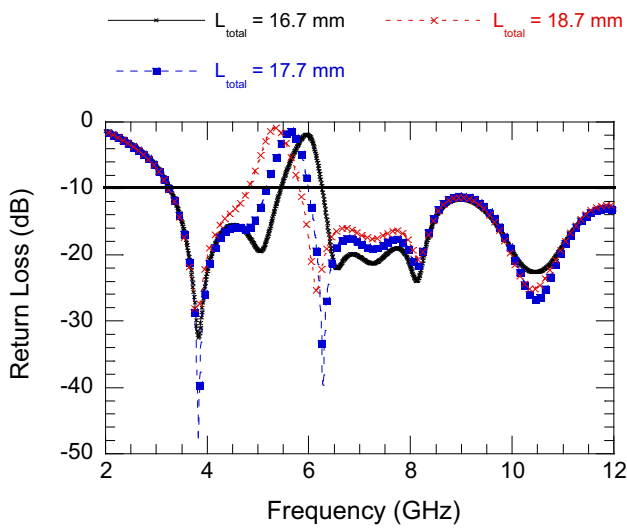


Fig. 5 Return loss for various lengths of L_{total_WLAN} of U-slot

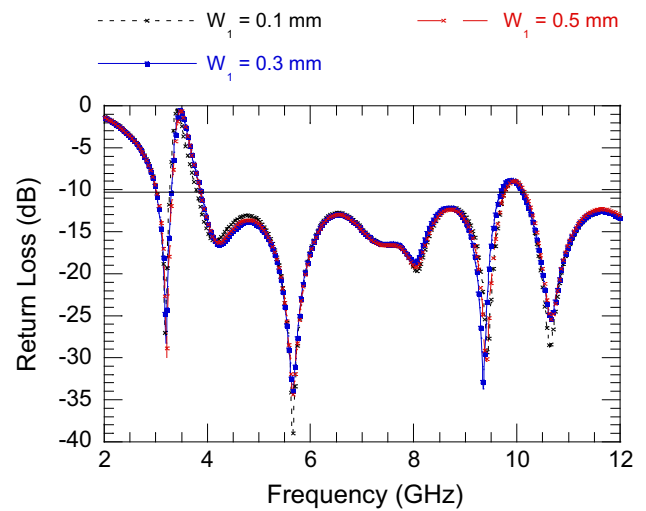


Fig. 8 Return loss for various width of U-slot

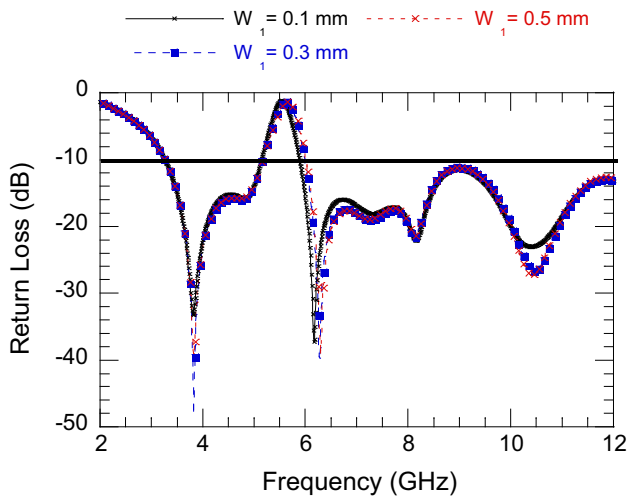


Fig. 6 Return loss for various width of U-slot

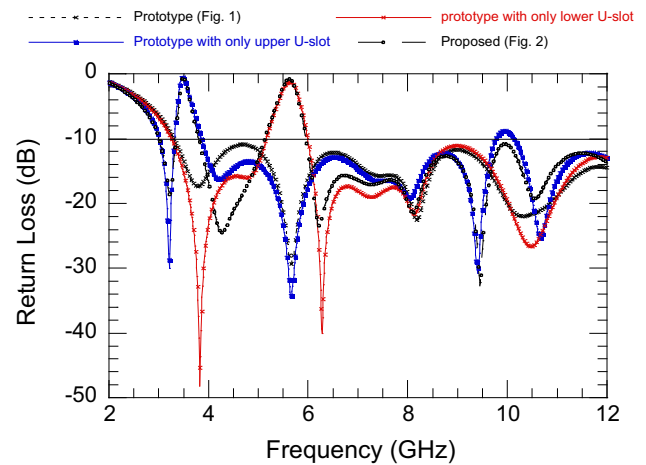


Fig. 9 Return loss characteristics of all configurations for comparisons

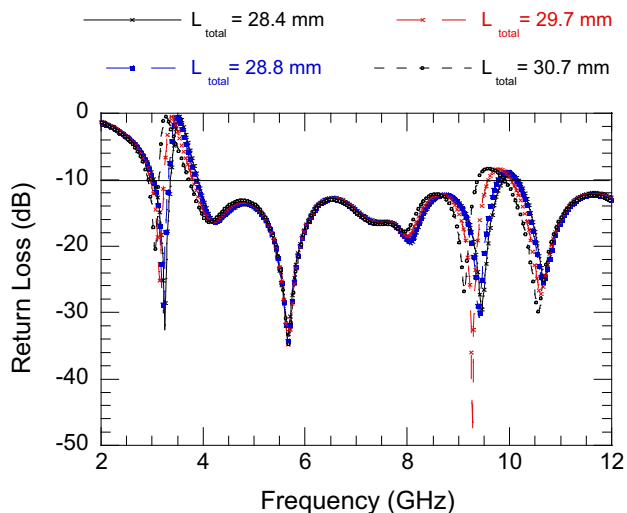


Fig. 7 Return loss for various lengths of L_{total_WiMAX} of U-slot

Furthermore to realize the WiMAX stop band in UWB region a second U-slot has been used in the same hexagonal patch. The return loss plots for various length and width are illustrated in Figs. 7 and 8 respectively. From the simulation result, it has been observed that in this case also the length has enough control for shifting and selecting the notch frequency. The return loss characteristics for all the configurations are illustrated in Fig. 9 for a comparison. The simulated return loss characteristics of the proposed antenna reveal stop bands of 0.5 GHz (3.3–3.8 GHz) and 0.78 GHz (5.15–5.93 GHz) over the UWB frequency span. Figure 10 also illustrates the return loss characteristics of the same antenna for various values of loss tangent. From the characteristics, it is observed that the peak value of return loss at notch frequency decreases while the loss tangent of the substrate increases.

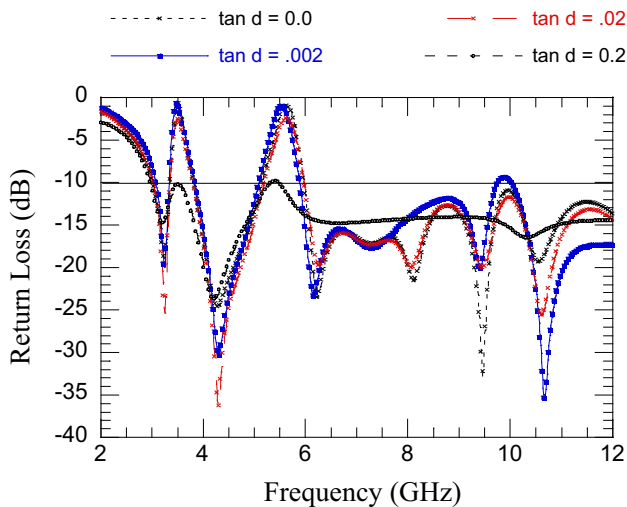


Fig. 10 Return loss characteristics for various value of loss tangent ($\tan d$)

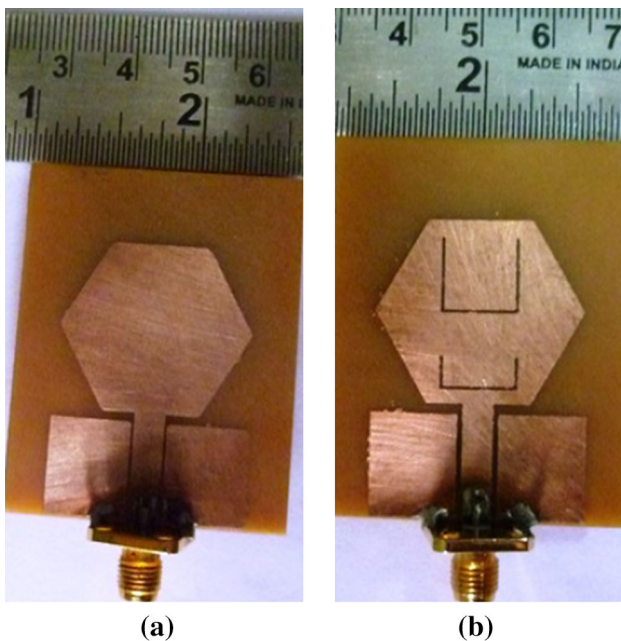


Fig. 11 Fabricated structure of (a) prototype, (b) proposed antenna

4 Experimental result

The photograph of the prototype and proposed fabricated antenna are shown in Fig. 11. The simulated and measured performances of prototype antenna (Fig. 11a) are plotted in Fig. 12 for a comparison. It is observed that from the plot the simulated response provides a BW of 10.37 GHz (3.15–13.52 GHz). The experimental response yields 10.54 GHz (3.06–13.60 GHz) impedance band. Thus good agreement between simulation and measurement is observed. The simulated and measured responses of the proposed antenna (Fig. 11b) are shown in Fig. 13. The simulated return loss

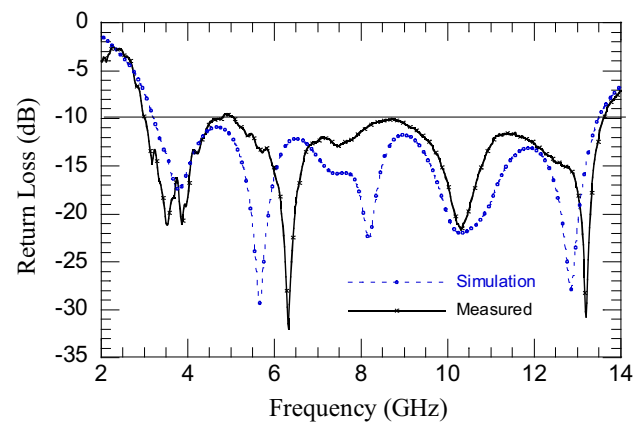


Fig. 12 Measured and simulated return loss of the prototype antenna

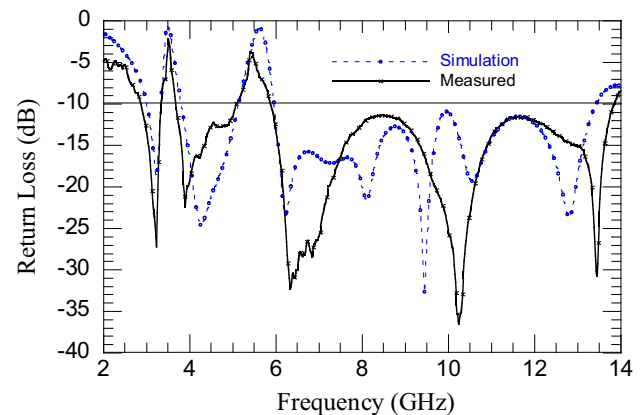


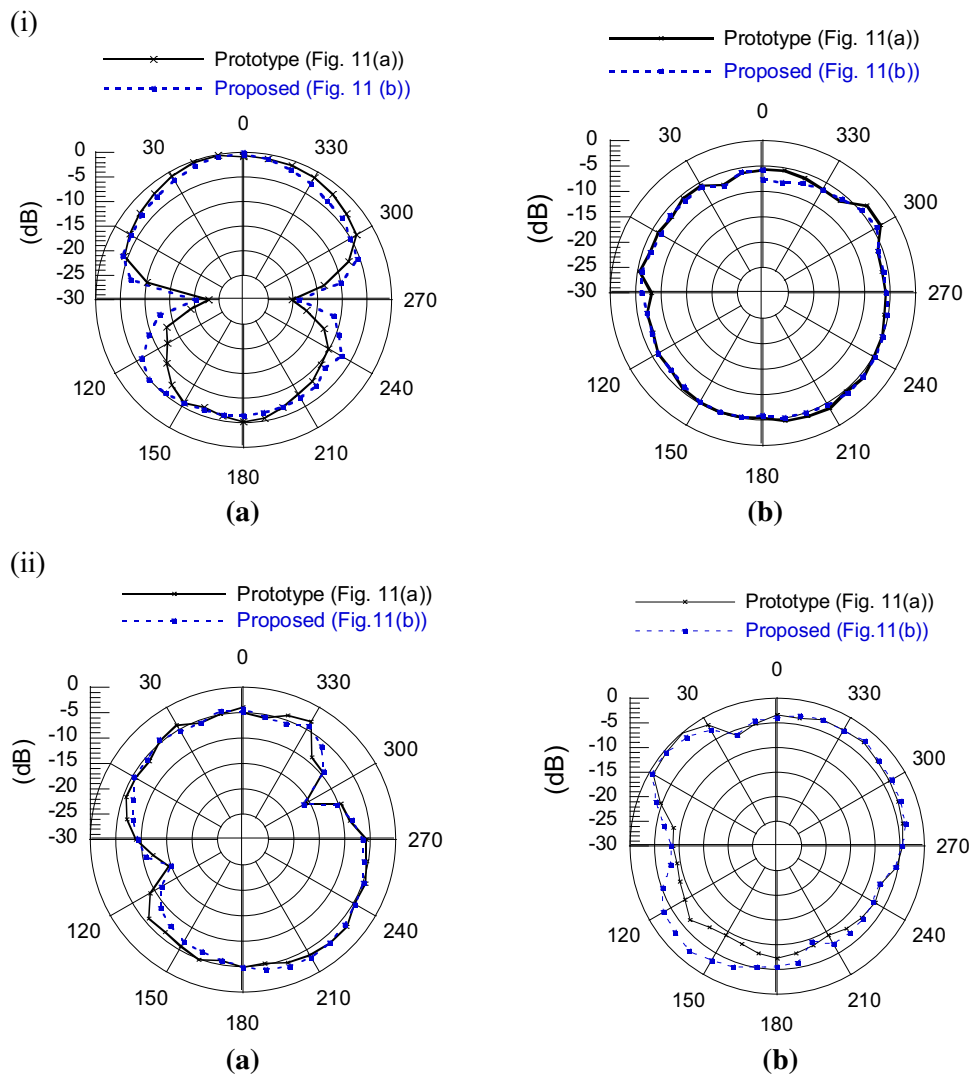
Fig. 13 Measured and simulated return loss of the proposed antenna

characteristic reveals stop bands of 0.5 GHz (3.3–3.8 GHz) and 0.78 GHz (5.15–5.93 GHz) for $-10 \text{ dB} \leq S_{11}$ within the frequency span from 3.1 to 13.43 GHz. The measured characteristic shows 0.4 GHz (3.3–3.7 GHz) and 0.78 GHz (5.12–5.9 GHz) stop bands which cover the entire WiMAX and WLAN band in the frequency span of 2.87–13.83 GHz.

5 Radiation pattern

Figure 14 shows the measured radiation patterns at 3.1 and 8.5 GHz. It can be observed that at the low frequency of 3.1 GHz, the radiation pattern in the H-plane is omnidirectional whereas in E-plane, it is figure of eight. At a higher frequency of 8.5 GHz, the radiation pattern is still approximately omnidirectional. H-plane radiation patterns are roughly the same as that of monopole antenna. From the characteristics, it is observed that the insertion of slots on the monopole plate of the antenna does not significantly alter the radiation patterns of the planar monopole antenna. The results of Fig. 14 show that the radiation patterns are reasonably stable

Fig. 14 Measured radiation pattern characteristics for prototype and proposed antenna. **i** at 3.1 GHz (a) E-plane pattern, (b) H-plane pattern. **ii** at 8.5 GHz (a) E-plane pattern, (b) H-plane pattern



throughout UWB. Thus it may be considered as good UWB antenna.

6 Input impedance, gain and efficiency

The real and imaginary parts of the input impedance versus frequency of prototype antenna is shown in Fig. 15. It is observed that the real part of the antenna impedance varies around 50Ω over the desired band, while its imaginary part has small values and fluctuates around zero. This is mainly because a continuous coupling is obtained between hexagonal patch and ground plane and hence a matching is achieved for different frequencies. Figure 16 shows the simulated input impedance of the proposed antenna. From the responses, it is observed that the impedance of the structure changes acutely making large reflection at 3.5 and 5.5 GHz which results in steep rise of return loss. In the notch bands, most of the power fed into the antenna is reflected back which leads to

a decrease of the radiation efficiency and hence the antenna gain. Simulated gain is plotted in Fig. 17. Two sharp drops occur at around 3.5 and 5.5 GHz as expected. The similar variation can be seen in the antenna efficiency curve plotted in Fig. 18. This characteristic can make sure the ability of the proposed antenna to reject the interference effectively. The proposed antenna gain varies from 2.6 to 6.4 dB over the whole operating range except in notch bands. It provides antenna efficiency more than 85 % except in notch bands.

7 Current distribution and analysis

Surface current distributions of the antenna with U-slots at different frequencies are shown in Fig. 19. At a pass band frequency, surface currents are passing through the patch but at notch band frequency, most of the surface currents are concentrated around the slot of the corresponding notch band. Therefore, slot stops the surface current and as a result notch

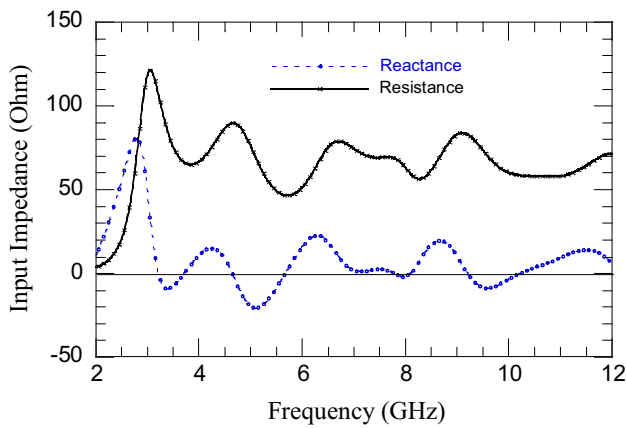


Fig. 15 Input impedance of prototype antenna

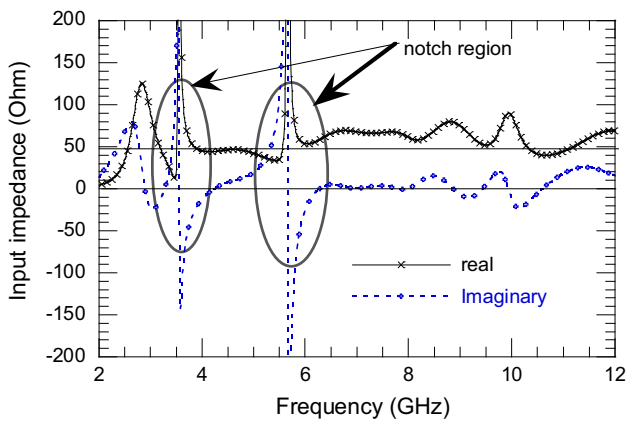


Fig. 16 Input impedance of proposed antenna

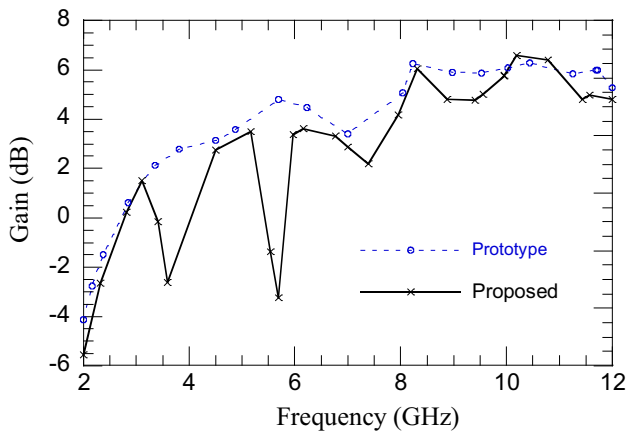


Fig. 17 Simulated gain versus frequency plot

band are created with negligible transmission. At a pass band frequency of 3.15 GHz (outside the notch band) the distribution of surface current is shown in Fig. 19a. In Fig. 19c at the notch frequencies (3.5 GHz), most of current distribution is clustered and oppositely directed on either side of the slot. The current has high intensity at the tip of the slot

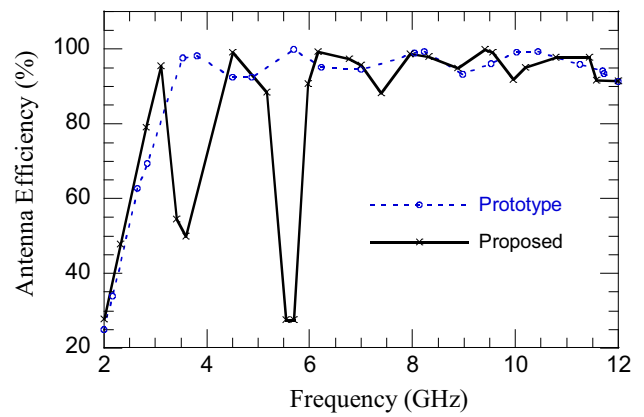


Fig. 18 Simulated antenna efficiency versus frequency plot

and low intensity at the middle point of the U-slot along its length. Consequently, top tip of the slot is modeled as a transmission line short circuit mode. The resultant equivalent load at the bottom of the slot is high impedance due to the length from the top to the bottom along the slot is approximately $\lambda/4$ at the corresponding frequency [20]. This high impedance at the feeding point leads to the desired impedance mismatch between the feed line and radiating patch. This phenomenon can be modeled as a quarter wavelength short circuit stub. Figure 19d shows the conceptual circuit model for proposed antenna, which has a series stub and antenna resistance (R_a). Stub1 works as a quarter wavelength transmission line terminated in a short circuited. It behaves as an open circuited series stub with high input impedance, causing a total impedance mismatch between the feed line and the radiating patch and so notch band generated. Similarly, at the second notch band stub 2 works similar to stub 1.

8 Transfer function and time domain study

Agilent make Vector Network Analyzer (N5230A) is used for transfer function measurement. A pair of proposed antennas is used as the transmitting and receiving antenna. The transmitter and receiver are positioned face to face with a distance of 160 mm. The measured magnitudes of S_{21} and group delay are shown in Fig. 20. It is observed that the variation of group delay for proposed antenna is almost constant across the whole UWB band except two notch bands, in which the maximum group delay is more than 11 ns in 3.5 GHz notch band and more than 10 ns in 5.5 GHz notch band. The magnitude of S_{21} is relatively flat (variation less than 10 dB) over the operating band except the notch bands. The measured phase of the transfer function is shown in Fig. 21. It is observed that the phase of S_{21} is relatively linear from 3 to 12 GHz excluding the notch bands. The measured group delay corresponds well to the phase of S_{21} , so it proves

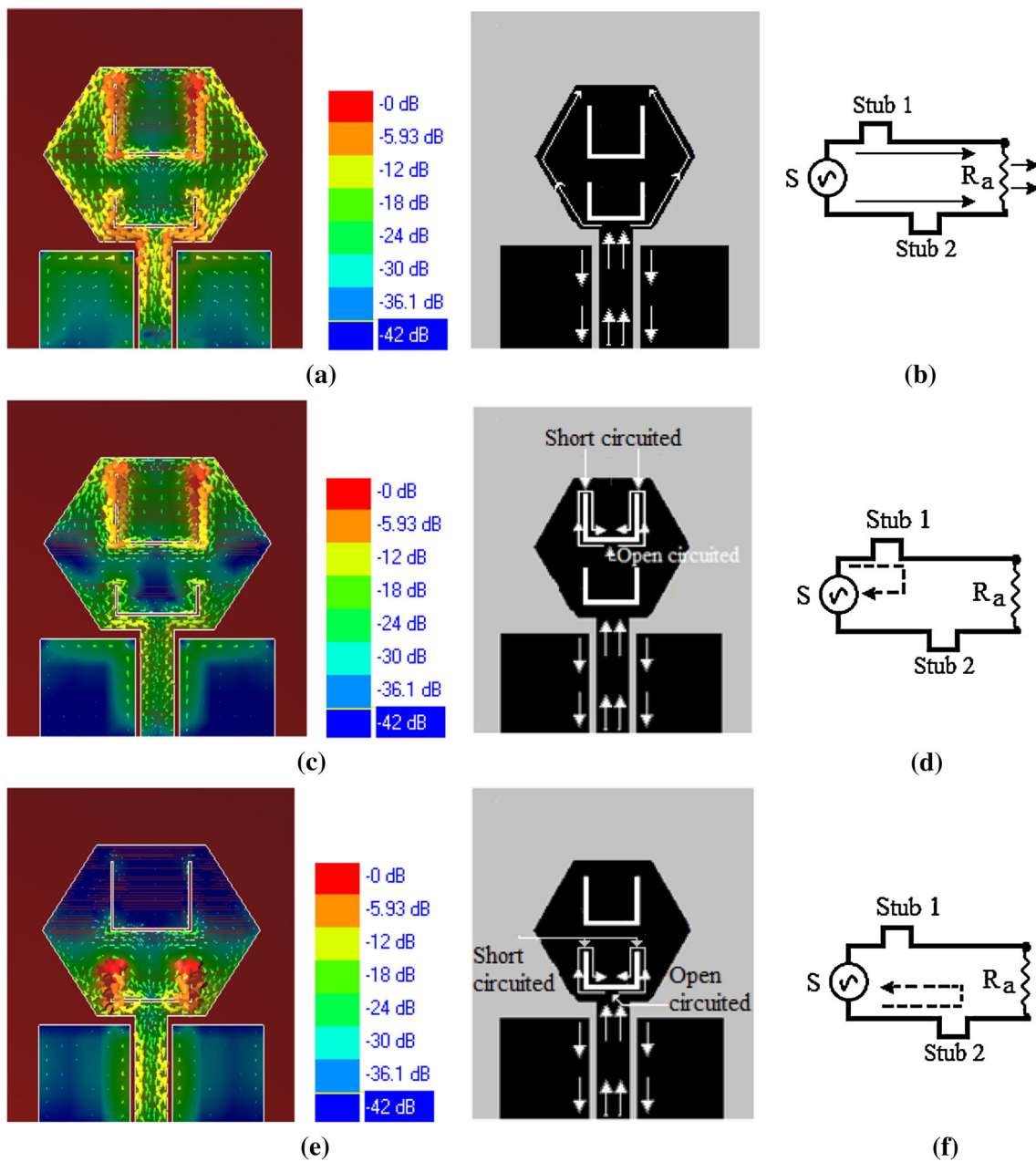


Fig. 19 Surface current distribution and conceptual model for antenna with U-slots at the pass band frequency 3.15 GHz in (a) and (b), at the first notch frequency 3.5 GHz in (c) and (d), at the second notch frequency 5.5 GHz in (e) and (f)

that the antenna has a good time-domain characteristic and a small pulse distortion as well.

9 Conclusions

To mitigate the interferences between the UWB systems and existing WiMAX, WLAN system, a CPW fed antenna with dual band rejection has been proposed. Parametric studies

of the antenna characteristics are presented. Dual stop bands are realised by etching a pair of U-slots inside hexagonal patch. Two types of band-notch structures extended from the prototype design are provided and verified. The surface current distributions are used to analyze the physical effect of the slot generating the band notch characteristics. This antenna has UWB performance with excellent WiMAX and WLAN rejection bands. Variation in the radiation patterns is very small over the UWB region except stop bands. It has

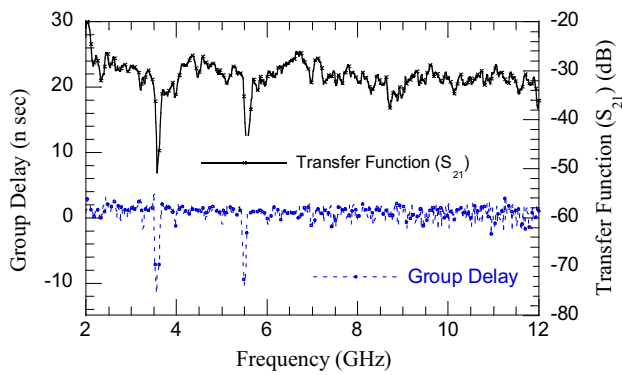


Fig. 20 The measured transfer function and group delay of the antenna systems

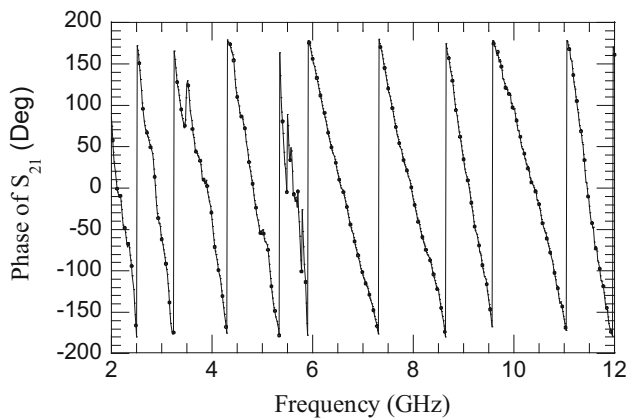


Fig. 21 The measured phase of S_{21} for proposed antenna systems

been revealed that the antenna has linear phase of transfer function and small group delay variation within the operating band except at notched bands which ensures the good linear transmission performances. Therefore, the proposed antenna is expected to be a good candidate in various modern UWB applications.

Acknowledgments This work was supported by AICTE, New Delhi, India.

References

1. First Report and Order. Revision of Part 15 of the Commission's Rule Regarding Ultra-Wideband Transmission system FCC 02–48. Federal Communications Commission (2002)
2. Ghaderi, M.R., Mohajeri, F.: A compact hexagonal wide slot antennas with microstrip fed monopole for UWB applications. *IEEE Antenna Wirel. Propag. Lett.* **10**, 682–685 (2011)
3. Azim, R., Islam, M.T., Mandeep, J.S., Mobashsher, A.T.: A planar circular ring ultra-wideband antenna with dual band-notched characteristics. *J. Electromagn. Waves Appl.* **26**(14–15), 2022–2032 (2012)
4. Chattopadhyay, K., Das, S., Das, S., Chaudhuri, S.R.B.: Ultrawide performances of printed hexagonal wideslot antenna with dual band notched characteristics. *Prog. Electromagn. Res. C* **44**, 83–93 (2013)
5. Mandal, T., Das, S.: Design of dual notch band UWB printed monopole antenna using electromagnetics band gap structure. *Microwave Opt. Technol. Lett.* **56**(9), 2195–2199 (2014)
6. Zhang, K., Wang, T., Cheng, L.L.: Analysis of band notched UWB printed monopole antennas using a novel segmented structure. *Prog. Electromagn. Res. C* **34**, 13–27 (2013)
7. Mandal, T., Das, S.: Ultra wide band printed hexagonal monopole antennas with WLAN band rejection. *Microwave Opt. Technol. Lett.* **54**, 1520–1525 (2012)
8. Shaalan, A.A.M., Ramadan, M.I.: Design of a compact hexagonal monopole antenna for ultra-wideband applications. *J. Infrared Milli Terahz Waves* **31**, 958–968 (2010)
9. Lin, Y.C., Hung, K.J.: Compact ultra-wide band rectangular aperture antenna and band-notched designs. *IEEE Trans. Antennas Propag.* **54**(11), 3075–3081 (2006)
10. Liang, J., Guo, L., Chiau, C.C., Chen, X., Parini, C.G.: Study of CPW-fed circular disc monopole antenna. *IEE Microwaves Antennas Propag.* **152**(6), 520–526 (2005)
11. Habib, M.A., Bostani Djaiz, A., Nedil, M., Yagoub, M.C.E., Denidni, T.A.: Ultra wideband CPW-fed aperture antenna with WLAN band rejection. *Prog. Electromagn. Res.* **106**, 17–31 (2010)
12. Li, P., Liang, J., Chen, X.: Study of printed elliptical/circular slot antennas for ultra-wide band applications. *IEEE Trans. Antennas Propag.* **54**(6), 1670–1675 (2006)
13. Roy, K.P., Tiwari, S.: Ultra wide band hexagonal monopole antennas. *IET Microwaves Antenna Propag.* **4**(4), 437–445 (2010)
14. Kim, K.H., Choi, D.H., Lee, S.S., Park, S.-O.: A miniature UWB planar monopole antenna with 5-GHz band-rejection filter and the time-domain characteristics. *IEEE Trans. Antennas Propag.* **54**(5), 1453–1460 (2006)
15. Qing, X., Chen, Z.N.: Compact coplanar waveguide-fed ultra-wideband monopole-like slot antenna. *IET Microwaves Antennas Propag.* **3**(5), 889–898 (2009)
16. Barbarino, S., Consoli, F.: UWB circular slot antenna with an inverted-L notch filter for the 5 GHz WLAN band. *Prog. Electromagn. Res.* **104**, 1–13 (2010)
17. Li, W.M., Ni, T., Quan, T., Jiao, Y.C.: A compact CPW fed UWB antenna with WiMAX band notched characteristics. *Prog. Electromagn. Res. Lett.* **26**, 79–85 (2011)
18. Sun, A.F., Yin, Y.Z., Jing, S.H., Yang, Y., Liu, B.W., Li, Z.: Broadband CPW-fed antenna with band-rejected characteristics for WLAN/WiMAX operation. *Prog. Electromagn. Res. C* **22**, 47–54 (2011)
19. Zeland IE3D™ software
20. Pozar, D.M.: Transmission line theory. In: *Microwave Engineering*, 3rd ed., pp. 49–90. Wiley, New York (2005)